TRANSNUCLEAR
AN AREVA COMPANY

DOCUMENT COVER SHEET

☒ Technical Report ☐ Other Technical Document

PROJECT NO:	10494	CLIENT:	Transnuclear, Inc.
DOCUMENT NUMBER:	E-21625-NP	ADDRESS (as required):	N/A

PROJECT NAME: High Burnup NUHOMS® 24/32PTH System

DOCUMENT TITLE: Thermal Testing of the NUHOMS® Horizontal Storage Module, Model HSM-H (Non-Proprietary)

SYSTEM, STRUCTURE, OR COMPONENT NAME (AS REQUIRED): Horizontal Storage Module Model HSM-H

SUMMARY DESCRIPTION:

The purpose of this report is to document the thermal testing of the HSM-H performed to validate the thermal analysis methodology employed in the design basis analysis of the HSM-H.

This Non-proprietary version is based on E-21625, rev. 1.

REVISION	TOTAL PAGES	PREPARER	VERIFIER	APPROVER	APPROVAL DATE
0	81	Jayant Bondre 4/14/05	U B Chopra 4/14/05	Jayant Bondre for Mike Mason	4/14/2005

REVISION CONTROL SUMMARY

REV.	DATE	DESCRIPTION	AFFECTED PAGES	AFFECTED DISKS
0	4/14/2005	Initial Issue	All	None

TABLE OF CONTENTS

LIST OF TABLES

LIST OF FIGURES

1.0 INTRODUCTION

1.1 Background

Recent demand for high heat load dry storage systems for nuclear spent fuel has led to the development of a new NUHOMS® Horizontal Storage Module (HSM) design, referred herein as the HSM Model H (HSM-H). The HSM-H has been developed for storage of high heat load spent fuel assemblies loaded in a Dry Shielded Canister (DSC) with decay heat loads of up to 40.8 kW. This HSM-H design is based on the proven design and extensive operational experience of the standardized NUHOMS® system HSM [3]. The principal components of the NUHOMS® system design consist of a reinforced concrete horizontal storage module (HSM) that contains a single stainless steel DSC. The DSC contains an internal basket structure that contains and supports the spent fuel assemblies. The HSM-H design incorporates design features and other improvements to provide enhanced heat rejection capability.

The HSM-H design is the basis for submittal to the NRC of a new license application and an amendment to an existing license for a high-heat load storage system [1] [2]. The predicted thermal performance of the HSM-H design for those license submittals is based on benchmarking of the models against test results for the standardized HSM module with a total heat load of 7 kW. The test results for the standardized HSM module are documented in the Pacific National Northwest Laboratory report PNL-7327 [4]. The tests demonstrated the conservatism in the HSM design analysis. However, since those tests are based on a total heat load of 7 kW, whereas the heat load for the recent license submittals are up to 40.8 kW, and since the design of the HSM-H incorporates new features and improvements that were not part of the testing on the standardized HSM, a new test program was undertaken. This report documents the thermal testing conducted on a full size mockup of the HSM-H for heat loads of up to 44 kW.

The main purpose of the test program conducted on the HSM-H design is to validate the thermal analysis methodology employed in the design basis analysis of the HSM-H, as documented in [1] and [2]. The analysis methodology consists of calculating the bulk temperatures in the HSM-H cavity and applying these bulk temperatures to an ANSYS model of the HSM-H to define convection boundary conditions to calculate DSC shell, HSM concrete, heat-shield and DSC support structure temperature.

The validity of the design methodology is evaluated based on a comparison of the measured temperatures from the DSC and HSM-H mockup with the temperatures predicted using the design basis methodology. The methodology to predict the temperatures of the mockup is the same as that used for the HSM-H design, except that appropriate differences with the test article are captured. The details of the mockup construction are provided in Section 3.1, while Section 3.2 describes the test instrumentation setup, Section 3.3 includes instrument calibration, accuracy and uncertainty estimates, Section 3.4 discusses the test conditions, and Section 3.5 presents the test plan and test sequence. The test results are presented in Section 4. A brief description of the design methodology and the predicted temperatures are presented in Section 5 and Section 6, respectively. The comparison between the measured and the predicted temperatures, and conclusions are discussed in Section 7.

The test was conducted by IONICS Inc. [13] at the Canonsburg facility in Pennsylvania. The testing included pre-testing of the DSC shell mockup by itself to verify that the strip heaters used to simulate the spent fuel decay heat were uniformly heating the circumference of the DSC shell mockup. The testing of the combined HSM-H and DSC mockups involved four runs at heat loads varying from 32 to 44 kW and with the design basis finned side heat shields. An additional three tests were run with flat, galvanized steel side heat shields to investigate the effectiveness of the fins, investigate the effectiveness of the slots in the support rail structure and the louvered top heat shield.

2.0 DESCRIPTION OF THE NUHOMS® SYSTEM WITH HSM-H

The NUHOMS® HSM-H is a free standing reinforced concrete structure designed to provide environmental protection, radiation shielding, and heat removal capability to ensure safe storage of spent fuel assemblies in a DSC.

The HSM-H design utilizes dual, independent inlet and outlet openings to allow buoyancy driven air to flow through its cavity. The concrete at the ceiling and the sidewalls are protected from direct radiation heat transfer from the hot surfaces of the DSC by heat shields. In the optional design for high heat loads, the side heat shields are finned and anodized. The top heat shield consists of louvers formed by angled aluminum plates. The louvered top heat shield permits air flow to pass through with little resistance, while blocking the majority of the radiated heat transfer from the DSC from reaching the concrete ceiling of the HSM-H.

The decay heat load from the stored canister is removed via a combination of radiation, free convection and conduction heat transfer. Buoyancy driven air flow within the HSM-H cavity is created by the temperature difference between the ambient air surrounding the HSM-H module and the DSC surface, and the height difference between the HSM-H inlet/outlet openings on the sidewalls. The airflow path through the HSM-H starts by the air being drawn in through the two screened openings at the bottom of the front face of the module and traveling along both sides of the module. See References [1] and [2] for more details on the NUHOMS® system with HSM–H. The air flow enters the HSM-H cavity by turning and passing under the module's side walls. Once in the cavity, the air flows upward around the DSC and the side heat shields before passing through the louvered heat shield at the top of the cavity. After exiting the louvered heat shield, the air flow turns horizontal and flows under the roof slab and over the top of the side walls, turns vertical to flow along the sides of the roof before finally exiting the module at the screened outlet vent opening. Figure 1 shows the air flow path in the internal cavity of the HSM-H design.

3.0 TEST SETUP

3.1 Test Mockup Hardware

The test mockup structure is designed to closely capture the geometry and flow resistance present for the flow of air through the HSM-H design, while conservatively bounding the heat losses through the simulated walls and roof of the HSM-H module. [[redacted]].

[[redacted]].

3.1.1 Description of the HSM-H Mockup

The mockup used to simulate the HSM-H module is a carbon steel structure which mimics the internal geometry of the HSM-H design with only a few changes (see Table 1), such as the distance between the inlet channels at the lower part of the HSM-H cavity. The inlet channels with the long cutouts are moved inwards, relative to the HSM-H design, to create a continuous and stable mockup sidewall.

[[redacted]].

The emissivities of the insulation materials Thermafiber® and Spin-Glas® have been measured for use in the analysis of the mockup [7 and 8, respectively]. The average of the measured emissivity values for the temperature range of interest is 0.85 for both materials.

The mockup of the top heat shield has the exact dimensions and shape as the design heat shield. Two types of side heat shields are utilized for testing. The first type is an aluminum backing plate supporting anodized aluminum fins. Only the heat shield surface facing the DSC (fins and backing plate) is anodized and the opposite surface facing the HSM-H walls remains as plain aluminum. The second type of side heat shield used in the test is fabricated from flat galvanized steel plates with the dimensions of the backing plate of the first type.

[[redacted]].

The support rails of the mockup, including the slotted bar and the round holes in the beams, are identical in geometry to the design support rails. The rail structure is supported by two cross beam assemblies that are independent of the mockup structure because the thin wall structure of the HSM-H mockup is not intended to carry the heavy weight of the support structure and the DSC mockup. In the actual HSM-H design, the support rails rest directly on the concrete structure of the HSM-H. Although the cross beam assemblies will present an additional resistance to the airflow within the HSM-H mockup, the location of the assemblies at the front and back of the cavity is such that the adverse impact is minimal.

[[redacted]].

The inlet and outlet vents of the HSM-H mockup are equipped with bird screens in the same manner as the HSM-H design. The geometry of the outlet vents matches that found in the HSM-H design for a stand-alone module.

3.1.2 Description of the DSC Mockup

The shell of the DSC mockup is fabricated of stainless steel and has the same inner and outer diameters, and the same cavity length as the NUHOMS®-32PTH DSC [2]. Since the thick shield plugs are not necessary for the DSC mockup, two thin, double disc, stainless steel plugs are constructed to cover the front and back of the DSC shell. The hollow space between the plug discs is filled with Thermafiber® insulation to reduce the direct axial heat transfer from the inner DSC cavity to the outer surface of the plugs. The back cover plug is welded to the DSC shell and the front cover plug is bolted to the DSC shell using a welded flange to provide access to the inner DSC cavity. The overall length of the DSC mockup is shorter than the designed NUHOMS®-32PTH DSC due to shorter cover plugs.

[[redacted]

[redacted]].

3.2 Test Instrumentation

A total of 108 thermocouples are used in the test, with 99 thermocouples installed in the interior of the mockup to capture the temperature profile of the DSC outer surface and the HSM-H inner surfaces. Instrumentation redundancy is provided by the symmetric placement of the thermocouples on the DSC and HSM-H surfaces and the expected symmetrical temperature profile about the vertical centerline. The opposite is also true in that the symmetric placement of the thermocouples can be used to verify the expected symmetry in the temperature profile.

[[redacted]

[redacted]

[redacted]].

Two thermocouples are installed outside the inlet vent screen, one inch from the center point to measure entering air temperature. The average measured temperature from these thermocouples is used as the assumed ambient temperature for the computational analysis of the mockup. Another 2 thermocouples are installed at the center point of the outlet screens and one inch inside the outlet vent to measure the exiting air temperature. This measurement is made to complete the heat balance and to verify the accuracy the flow resistance calculation. The calculation of the air flow resistance is the initiating part of the computational analysis.

Four thermocouples are located at the outer surface of the HSM-H mockup in order to calculate the heat loss through the mockup walls and roof. These thermocouples are located between the Thermafiber® insulation boards, 4 inch from the outer surface. One thermocouple measures the ambient temperature as a redundant value for the entering air temperature and to calculate the heat losses. [redacted]]. The calculation of heat losses through mockup outer surfaces is presented in APPENDIX E.

A control panel provides uniform electric load to the strip heaters installed within the DSC shell. The required load is set digitally on the panel. An indicator shows the total electrical load supplied to the heaters. [[redacted]].

3.3 Instrument Calibration, Accuracy and Uncertainty Estimates

Temperature measurement uncertainty is produced by the thermocouples, extension wires, and data acquisition system. Each component in the temperature measurement chain adds to the overall uncertainty. The overall uncertainty is equal to the square root of the sum of the squares of the individual temperature measurement uncertainties. The individual uncertainties are:

Max. Measured Temperature = 409°F
Thermocouple: [redacted]
Extension wire:

Data Acquisition System:

The total temperature measurement uncertainty is:
[redacted]

The accuracy of the power controller panel is [redacted] of the full scale. For the maximum heat load of 44 kW in the test, the maximum uncertainty of the power panel is:

[redacted]

3.4 Test Conditions and Location

The mockup is located indoor in a large fabrication hall, approximately 78 ft wide, 80 ft high, and 1,000 ft long. The inlet vents are about 10 ft away from the closest wall. No extra heat source was present close to the mockup during the test. Since all the outer surfaces of the mockup are insulated, the effect of surrounding objects on the test is minimal.

3.5 Test Plan

3.5.1 Uniform Heat Verification Test of the DSC Shell

A primary assumption in the computational analysis of the HSM-H mockup is that the heating from the electrical strip heaters is uniformly distributed over the inner surface of the DSC shell. The electro-mechanical setup of the heaters theoretically provides a uniform heat distribution.

The uniformity of the heat load generated by the strip heaters was verified via the pre-testing of the DSC shell mockup. [[redacted]].

To ensure the correctness of the heaters' setup, a verification test was conducted on the DSC mockup prior to its installation inside the HSM-H mockup. The verification test consisted of two test runs in both vertical and horizontal DSC orientations. The DSC was supported off the concrete floor using two sections of 4"×4" square tubing. The bolted cover plate was facing the floor during the vertical test. At each orientation a test run was conducted at heat loadings of 32 and 40 kW heat loads.

[[redacted]

[redacted]

[redacted].

[[redacted]].

3.5.2 Verification Tests of Modeling Methodology

After the uniform heat verification testing of the DSC mockup, a series of thermal tests were conducted to obtain data by which to verify the modeling methodology used to simulate the combined thermal performance of the DSC and HSM-H module. The tests were conducted with the finned side heat shields at four heat loads, 32, 36, 40, and 44 kW. Three additional tests were conducted to investigate the effectiveness of some of the specific features of HSM-H heat shields and DSC support structure. One test was with the un-finned side heat shields at 32 kW to evaluate the effect of the finned verses un-finned side heat shield on the thermal performance of the HSM-H. Another test was conducted to investigate the effectiveness of the slots in the DSC support rail structure. A third test was conducted to investigate the effectiveness of the louvered top heat shield versus a flat plate for the top heat shield. .

Each test is run to steady state conditions. [[redacted]].

4.0 Test Results

4.1 Results of the Uniform Heat Verification Test

The thermocouple readings measured during the uniform heat verification testing are shown in Table 2 through Table 5. [[redacted]]

[[redacted]].

In conclusion, based on the data adjustments presented above, the heat load has been shown to be uniform over the inner shell of the DSC mockup to within an acceptable range. Therefore, it is valid to assume that uniform heat loading is also present during for the combined DSC and HSM-H mockup testing.

4.2 Results of the Mockup Testing

The tests are run to steady state conditions, where a steady state condition is defined as being reached when the slopes of the temperature curves are less than ±1°F over a two hour period. This steady state criterion was achieved during each of the test runs by all but 3 or 4 of 108 thermocouples. Only four thermocouples in the 32 kW test (TC# 18, 26, 103, and 107) and three thermocouples in the 40 kW test (TC# 18, 26, and 107) show curve slopes larger than ±1°F, with the greatest variation being ±3°F. Because thermocouples 103 and 107 are located outside the HSM-H mockup cavity, the slightly larger temperature slope of these thermocouples is suspected of being caused by the variation in the ambient temperature during the data recording period.

Given the small number of thermocouples with temperature slopes larger than ±1°F and the fact that their recorded slopes are only slightly higher than the criteria of ±1°F, it is valid to conclude that steady state conditions were indeed achieved during the recording periods.

Typical recorded temperature curves are shown in Figure 13 and Figure 14 for the various heat loads tested. The measured temperatures of each thermocouple during a two hour period at steady state conditions are averaged to rectify the small fluctuations in the temperature readings. These average temperatures are reported as the steady state temperatures. The steady state temperatures for the mockup testing conducted at 32, 36, 40, and 44 kW heat loads, and for three additional tests which investigated the effectiveness of some geometry features of heat shields and DSC support structures are listed in APPENDIX A Tables A-1 through A-7.

5.0 DESCRIPTION OF DESIGN BASIS THERMAL ANALYSIS METHODOLOGY FOR NUHOMS® SYSTEM WITH HSM-H

The thermal performance of the HSM-H storage modules is based on a computational methodology described in detail in the SARs for the NUHOMS® system [1 and 2]. The methodology used is similar to that used for the standardized NUHOMS® HSM system [3], which is a proven design with extensive operational experience. Since the basic heat transfer mechanism involved with both designs are the same, the basic methodology, with the appropriate modifications to reflect the design changes, should be applicable to each design. This is true even though the heat loading associated with the HSM-H design could be 70% or greater than the current heat load for the standardized NUHOMS® design since the methodology is based on first principles of heat transfer that scale with temperature level and heat loads.

However, because the heat loads associated with the HSM-H design represent a substantial increase over the heat loads for which the standardized NUHOMS® HSM system has been validated, it is desirable to evaluate the computational design methodology and demonstrate its validity at higher heat loads via physical testing. A full scale mockup of the HSM-H and the NUHOMS® 32PTH DSC are utilized in the thermal test. The mockup represents the inner dimensions of the HSM-H design in a 1:1 scale.

5.1 Description of the Analysis Methodology

The computational analysis consists of two steps. In the first step, the energy balance and hydraulic equations are combined to calculate the bulk air temperatures in the HSM-H cavity. In the second step, the calculated bulk air temperatures are applied in an ANSYS model of the combined DSC and HSM-H module to define the convection boundary conditions.

The energy balance and hydraulic equations used in the first step are:

$$Q = \dot{m}_E\, C_p\, (T_{exit} - T_c) = \dot{m}_E\, C_p\, \Delta T_{HSM} \qquad \textit{Energy Balance}$$

$$\Delta P_s = (\frac{g}{g_c})(\rho_c - \rho_s)(\Delta h) = (\frac{g}{g_c})(\Delta\rho)(\Delta h) \qquad \textit{Stack Pressure (Buoyancy)}$$

$$\Delta P_{loss} = \sum(K \cdot \frac{1}{2} \cdot \rho \cdot \frac{V^2}{g_c}) = \sum(K_{Ei} \cdot \frac{1}{2} \cdot \frac{1}{gc \cdot \overline{\rho}} \cdot \frac{\dot{m}_{Ei}^{\,2}}{A_{Ei}^{\,2}}) \qquad \textit{Dynamic Loss}$$

The entering air temperature and the total heat load (Q) are inputs to the equations. Assuming a linear, progressive temperature rise around the DSC shell, an iterative solution of the above equations is employed to determine the bulk temperatures within the HSM-H cavity which satisfies all three equations simultaneously.

The convection coefficients for the HSM-H mockup are calculated using the same correlations and macros described in the SARs of the NUHOMS® HD system and Amendment 8 of the standardized NUHOMS® system [7] [1]. Since the HSM-H mockup is located indoors, no solar heat load is considered in the analysis.

The heat loading for the DSC mockup is applied as a uniform heat flux over the radial inner surface of the DSC mockup. The radiation heat transfer within the HSM-H cavity is modeled using the ANSYS /AUX12 processor via super element MATRIX50 [9].

5.2 Prediction of the Mockup Temperatures

A finite element model of the mockup was developed using the ANSYS computer code [9]. The model simulates one-half of the test setup with symmetry conditions assumed about the vertical centerline of the mockup. The model captures the exact geometry of the mockup as defined in the mockup fabrication drawings [10]. Where possible, the nodes of the ANSYS model were placed at the same location as the thermocouple placement so that the predicted thermocouple temperatures could be retrieved directly from the model. In the few instances where no model node was available at a specific thermocouple location, linear interpolation using neighboring nodes was used to establish the equivalent temperature at the thermocouple location.

The thermal properties for the stainless steel, carbon steel, and aluminum used in the mockup fabrication are taken from the ASME code [11]. The emissivity values for plain aluminum, anodized aluminum, and stainless steel are 0.1, 0.8, and 0.46, respectively. An emissivity value of 0.587 is used for the DSC shell to be consistent with Reference [1]. These values are identical to values used in the design basis analysis. An emissivity of 0.25 is assumed for the galvanized steel plate. The emissivities of the insulation materials are measured independently from representative material samples using a hemispherical directional reflectance (HDR) method. The emissivity measurements were conducted by Surface Optic Corporation located in San Diego, CA. [7 and 8] and the results are summarized in APPENDIX C.

The methodology used to define the boundary conditions of the finite element model is identical to that described in the SARs of the NUHOMS® HD system and Amendment 8 of the standardized NUHOMS® system [1] and [2]. This methodology is described briefly in Section 5.1. The results obtained from the ANSYS mockup model for the various test conditions are summarized in APPENDIX B.

It should be noted that the results presented in APPENDIX B differ from the pre-test predictions submitted to NRC for their review and use [12]. The differences arise from the fact that the predicted temperatures submitted to NRC were generated prior to finalizing the test setup. [[redacted]]. Further, the calculations in [12] assumed an ambient temperature of 70°F. In contrast, the temperatures shown in APPENDIX B are predicted based on the final placement of the thermocouples and the actual ambient temperature as measured at the time of the test.

The APPENDIX B results also include the following modifications to the assumptions and methodology used in Reference [12]. These modifications are described in detail in [1]:

1. The assumption of flat plate for modeling the top louvered heat shield has been revised to model the actual geometry of the louvered top heat shield.

2. Stack height is now set equal to the HSM-H cavity height. Stack height was previously the height difference between the inlet and outlet vents.

3. The emissivity of 0.587 is used for the DSC shell instead of 0.46 used in Reference [12].

4. The convection correlation used for the top 22.5° segment of the DSC shell is for a heated flat-plate-facing-up to account for turbulence.

5. The following loss coefficients which were neglected in Reference [12] analysis for calculation of exit air temperature are now added to the model:

   A second contraction and a change of flow direction including the resulting friction losses are added to the inlet channel (first region) after the v-shape channel. A loss coefficient corresponding to the direction change after the discharge of flow to HSM-H cavity is also added to second region.

6. The convection boundary conditions around the DSC shell now use the following air temperature for convection:

   Various bulk temperatures around DSC and within HSM-H cavity (T_0 to T_8) are replaced by entering air temperature (T_{amb}), or exit air temperature (T_{exit}), or average air temperature (T_{mean}) as applicable. The average air temperature is the arithmetic average of T_{exit} and T_{amb}.

6.0 TEST AND ANALYSIS RESULTS COMPARISON

The measured and the predicted temperatures are compared in Table 6 through Table 13, based on the location of the thermocouples. Where ever a redundant thermocouple location exists, an average temperature value is computed and reported. The redundant thermocouples are those located on opposite sides of the HSM-H vertical symmetry plane (i.e., between the 90 - 270° locations as illustrated in Figure 8).

The results presented in the tables show that, generally, the DSC shell temperatures are predicted with considerable conservatism, with the conservatism in the HSM-H wall temperature predictions less than the conservatism involved in DSC shell temperature predictions. There is generally good agreement between the measured and predicted side heat shield temperatures.

The following summarizes the differences observed between the measured and the predicted values with a brief discussion where needed:

- The predicted shell temperatures at the top of the DSC are [[redacted]] higher than the measured values.
- The difference between the predicted and the measured DSC shell temperatures are[[redacted]] at the 225 or 315 degree locations*.
- The HSM-H floor temperatures are over-predicted by [[redacted]] from the measured values.
- [redacted]The predicted temperatures at the ceiling of the HSM-H are [redacted]] higher than the measured values. [[redacted]

[redacted]

---

* See Figure 7 for orientation

[redacted] [redacted]] the predicted temperatures at the ceiling of the HSM-H are [[redacted]] higher than the measured values.

- The predicted HSM-H sidewall temperatures are [[redacted]] higher than the measured values.
- The predicted temperatures for the front and backwalls are [[redacted]F] higher than the measured values.
- The predicted temperatures for the side heat shield are [[redacted]] higher than the measured values.
- The predicted temperatures at the top heat shield are approximately [redacted]] higher than the measured values. See the reason given for the negative values for the HSM-H ceiling above.
- The predicted exit air temperature is within close agreement with the measured values (TC 102 & TC 103).

The assumptions used for convective heat transfer from the DSC surface results in conservative prediction of DSC shell temperatures at the top and bottom portions of the DSC as shown in Table 6 through Table 13. This over prediction on the DSC shell temperature occurs because credit is not taken for all of the turbulent heat transfer at the top of the DSC shell. At the bottom of the DSC shell, the amount of over prediction is because the support rails provide a better conduction path than that captured in the analysis model. This also explains the over prediction in the HSM concrete and the heat shield temperatures.

To evaluate the effectiveness of the finned side heat shield, the results of the finned side heat shield, (Table 6), are compared with the un-finned side heat shield, (Table 10), for the same 32 kW heat load. The evaluation, when accounting for the difference in ambient temperature during test conditions, (Table 6 data with 81°F ambient vs. Table 10 data with 61.5°F ambient) shows that the finned side heat shields decrease the DSC shell temperatures by approximately [redacted]]. Similarly, the HSM side wall, front and back walls, and the HSM ceiling temperatures decrease by less than [[redacted]] side heat shields is an acceptable alternative.

To evaluate the effectiveness of the slots in the slotted DSC support rails, the measured temperatures with the slotted DSC support rails (Table 10) are compared with the slots fully plugged in DSC support rails (Table 12), for the same 32 kW heat load and same side heat shield (un-finned) geometry and same top heat shield (louvered) geometry. The evaluation shows that as expected, plugging the slots increases the DSC shell temperature at the bottom by approximately [[redacted]] and the temperatures at the DSC top, side walls, top portion, front and back wall top portions decrease slightly. Temperatures at other locations had insignificant impact. Therefore, it can be concluded that plugging the slots in the DSC support rail does not alter the thermal performance of the HSM-H module.

To evaluate the effectiveness of the louvered top heat shield, the measured temperatures with the louvered top heat shield (Table) are compared with the flat top heat shield (Table), for the same 32 kW heat load and same side heat shield (un-finned) geometry and plugged slots in the slotted DSC support rails. The evaluation shows that as expected, the flat top heat shield reduced the HSM ceiling temperatures by approximately [[redacted]] when compared with the louvered top heat shield after accounting for the difference in ambient temperature during test conditions. The effect on the side, front and back wall top portions was an increase of [[redacted]] and the DSC shell temperatures had even smaller effect than concrete. Therefore it can be concluded that the thermal performance of the HSM-H is approximately equal with both the flat top heat shield and louvered top heat shield while the flat top heat shield is slightly better than the louvered top heat shield for ceiling temperature.

7.0 CONCLUSIONS

The results presented in Section 6.0 demonstrate that the revised analytical methodology described in [1] conservatively predicts the peak DSC temperatures, the peak HSM-H concrete, and the top and side heat shield temperatures.

[[redacted]

[redacted]]

Since the predicted DSC shell temperatures from the HSM-H ANSYS model are used to evaluate the DSC basket components and fuel cladding temperature in the DSC detail model, a large conservatism in the DSC shell temperatures translates in a large conservatism in predicting the DSC basket components and fuel cladding temperatures.

8.0 References

1. Safety Analysis Report for NUHOMS®-24PTH, Rev. 4, Amendment 8 to Standardized NUHOMS® Horizontal Modular Storage System for Irradiated Nuclear Fuel, NUH-003, Docket No. 72-1004.

2. Safety Analysis Report for NUHOMS® HD Horizontal Modular Storage System for Irradiated Nuclear Fuel, Rev. 0, Docket No. 72-1030.

3. Final Safety Analysis Report for the Standardized NUHOMS®-Horizontal Modular Storage System for Irradiated Nuclear Fuel, NUH-003.0103, Revision 8, June 2004.

4. NUHOMS® Modular Spent Fuel Storage System: Performance Testing, Report PNL 7327/UC-812/EPRI NP-6941, Pacific Northwest Laboratory & Carolina Power and Light Company, September 1990.

5. Johns Manville Corporation, Spin-Glas® 814 Series, Technical Data – Attached to APPENDIX D

6. Thermafiber Corporation, Thermafiber® Industrial Board, Technical Specification – Attached to APPENDIX D.

7. Surface Optic Corporation, Emissivity Test Report for Thermafiber®, Report No. SOC-R-1275MP-001-1203, "Hemispherical Directional Reflectance (HDR) Measurements on Four (4) Sample Coupons (Insulation Material, Samples A, B, C, and D)"

8. Surface Optic Corporation, Emissivity Test Report for Spin-Glas®, Report No. SOC-R-1281MP-001-0104, "Hemispherical Directional Reflectance (HDR) Measurements on Transnuclear Samples E, F, G, and H"

9. ANSYS Computer Code and User's Manuals, Rev. 8.0.

10. Ionics Corporation, Thermal Test Mockup Drawings TT-1 toTT-14, Latest Revision, Project No. 1383, approved by TN, document no. E-20650, and E-20725

11. ASME Boiler and Pressure Vessel Code, Section II, Part D, "Material Properties", 1998 and 2000 addenda

12. Transnuclear submitted to NRC dated August 16, 2004, Subject: "Thermal Test Calculation for NUHOMS® HSM-H Docket No. 72-1030 and 72-1004 Amendment 8", with enclosed calculation 10494-62, Rev. 0, "Pretest Prediction of the Thermocouple Temperatures for the HSM-H Thermal Testing" [PROPRIETARY].

13. Ionics, Incorporated, Bridgeville Division, 30 Curry Avenue, Canonsburg, PA .

Table 1
Comparison of the Mockup and the HSM-H Design

[redacted]	[redacted]	[redacted]
[redacted]	[redacted]	[redacted]
[redacted]	[redacted]	[redacted]
[redacted]	[redacted]	[redacted]
[redacted]	[redacted]	[redacted]
[redacted]	[redacted]	[redacted]
[redacted]	[redacted]	[redacted]

Table 2 Measured Values for the Vertical Verification Test, 32 kW Heat Load

[redacted]	[redacted]	[redacted]	[redacted]	[redacted]	[redacted]	[redacted]
[redacted]	[redacted]	[redacted]	[redacted]	[redacted]	[redacted]	[redacted]
	[redacted]	[redacted]	[redacted]	[redacted]	[redacted]	[redacted]
[redacted]	[redacted]	[redacted]	[redacted]	[redacted]	[redacted]	[redacted]
	[redacted]	[redacted]	[redacted]	[redacted]	[redacted]	[redacted]
[redacted]	[redacted]	[redacted]	[redacted]	[redacted]	[redacted]	[redacted]

[redacted]	[redacted]		[redacted]		[redacted]
[redacted]	[redacted]	[redacted]	[redacted]	[redacted]	[redacted]

Table 3 Measure Values for the Vertical Verification Test, 40 kW Heat Load

[redacted]	[redacted]	[redacted]	[redacted]	[redacted]	[redacted]	[redacted]
[redacted]	[redacted]	[redacted]	[redacted]	[redacted]	[redacted]	[redacted]
	[redacted]	[redacted]	[redacted]	[redacted]	[redacted]	[redacted]
[redacted]	[redacted]	[redacted]	[redacted]	[redacted]	[redacted]	[redacted]
	[redacted]	[redacted]	[redacted]	[redacted]	[redacted]	[redacted]
[redacted]	[redacted]	[redacted]	[redacted]	[redacted]	[redacted]	[redacted]

[redacted]	[redacted]		[redacted]		[redacted]
[redacted]	[redacted]	[redacted]	[redacted]	[redacted]	[redacted]
[redacted]	[redacted]	[redacted]	[redacted]	[redacted]	[redacted]
[redacted]	[redacted]	[redacted]	[redacted]	[redacted]	[redacted]
[redacted]	[redacted]	[redacted]	[redacted]	[redacted]	[redacted]
[redacted]	[redacted]	[redacted]	[redacted]	[redacted]	[redacted]
[redacted]	[redacted]	[redacted]	[redacted]	[redacted]	[redacted]
[redacted]			[redacted]	[redacted]	[redacted]

Table 4 Measured Values for the Horizontal Verification Test, 32 kW Heat Load

[redacted]	[redacted]	[redacted]	[redacted]	[redacted]	[redacted]	[redacted]
[redacted]	[redacted]	[redacted]	[redacted]	[redacted]	[redacted]	[redacted]
	[redacted]	[redacted]	[redacted]			
	[redacted]	[redacted]	[redacted]			
	[redacted]	[redacted]	[redacted]			
	[redacted]	[redacted]	[redacted]			
[redacted]	[redacted]	[redacted]	[redacted]	[redacted]	[redacted]	[redacted]
	[redacted]	[redacted]	[redacted]			
	[redacted]	[redacted]	[redacted]			
	[redacted]	[redacted]	[redacted]			
	[redacted]	[redacted]	[redacted]			
	[redacted]	[redacted]	[redacted]			
	[redacted]	[redacted]	[redacted]			
	[redacted]	[redacted]	[redacted]			
[redacted]	[redacted]	[redacted]	[redacted]	[redacted]	[redacted]	[redacted]
	[redacted]	[redacted]	[redacted]			
	[redacted]	[redacted]	[redacted]			
	[redacted]	[redacted]	[redacted]			
	[redacted]	[redacted]	[redacted]			
	[redacted]	[redacted]	[redacted]			
	[redacted]	[redacted]	[redacted]			
	[redacted]	[redacted]	[redacted]			
[redacted]	[redacted]	[redacted]	[redacted]	[redacted]	[redacted]	[redacted]
	[redacted]	[redacted]	[redacted]			
	[redacted]	[redacted]	[redacted]			
	[redacted]	[redacted]	[redacted]			
	[redacted]	[redacted]	[redacted]			
	[redacted]	[redacted]	[redacted]			
	[redacted]	[redacted]	[redacted]			
	[redacted]	[redacted]	[redacted]			
[redacted]	[redacted]	[redacted]	[redacted]	[redacted]	[redacted]	[redacted]
	[redacted]	[redacted]	[redacted]			
	[redacted]	[redacted]	[redacted]			
	[redacted]	[redacted]	[redacted]			
	[redacted]	[redacted]	[redacted]			

[redacted]	[redacted]		[redacted]		[redacted]	[redacted]	[redacted]
[redacted]	[redacted]	[redacted]	[redacted]	[redacted]	[redacted]	[redacted]	[redacted]
[redacted]	[redacted]	[redacted]	[redacted]	[redacted]	[redacted]	[redacted]	[redacted]
[redacted]	[redacted]	[redacted]	[redacted]	[redacted]	[redacted]	[redacted]	[redacted]
[redacted]	[redacted]	[redacted]	[redacted]	[redacted]	[redacted]	[redacted]	[redacted]
[redacted]	[redacted]	[redacted]	[redacted]	[redacted]	[redacted]	[redacted]	[redacted]

Table 5 Measured Values for the Horizontal Verification Test, 40 kW Heat Load

[redacted]	[redacted]	[redacted]	[redacted]	[redacted]	[redacted]	[redacted]
[redacted]	[redacted]	[redacted]	[redacted]	[redacted]	[redacted]	[redacted]
	[redacted]	[redacted]	[redacted]			
	[redacted]	[redacted]	[redacted]			
	[redacted]	[redacted]	[redacted]			
	[redacted]	[redacted]	[redacted]			
[redacted]	[redacted]	[redacted]	[redacted]	[redacted]	[redacted]	[redacted]
	[redacted]	[redacted]	[redacted]			
	[redacted]	[redacted]	[redacted]			
	[redacted]	[redacted]	[redacted]			
	[redacted]	[redacted]	[redacted]			
	[redacted]	[redacted]	[redacted]			
	[redacted]	[redacted]	[redacted]			
	[redacted]	[redacted]	[redacted]			
[redacted]	[redacted]	[redacted]	[redacted]	[redacted]	[redacted]	[redacted]
	[redacted]	[redacted]	[redacted]			
	[redacted]	[redacted]	[redacted]			
	[redacted]	[redacted]	[redacted]			
	[redacted]	[redacted]	[redacted]			
	[redacted]	[redacted]	[redacted]			
	[redacted]	[redacted]	[redacted]			
	[redacted]	[redacted]	[redacted]			
[redacted]	[redacted]	[redacted]	[redacted]	[redacted]	[redacted]	[redacted]
	[redacted]	[redacted]	[redacted]			
	[redacted]	[redacted]	[redacted]			
	[redacted]	[redacted]	[redacted]			
	[redacted]	[redacted]	[redacted]			
	[redacted]	[redacted]	[redacted]			
	[redacted]	[redacted]	[redacted]			
	[redacted]	[redacted]	[redacted]			
[redacted]	[redacted]	[redacted]	[redacted]	[redacted]	[redacted]	[redacted]
	[redacted]	[redacted]	[redacted]			
	[redacted]	[redacted]	[redacted]			
	[redacted]	[redacted]	[redacted]			
	[redacted]	[redacted]	[redacted]			

[redacted]	[redacted]		[redacted]		[redacted]	[redacted]	[redacted]
[redacted]	[redacted]	[redacted]	[redacted]	[redacted]	[redacted]	[redacted]	[redacted]
[redacted]	[redacted]	[redacted]	[redacted]	[redacted]	[redacted]	[redacted]	[redacted]
[redacted]	[redacted]	[redacted]	[redacted]	[redacted]	[redacted]	[redacted]	[redacted]
[redacted]	[redacted]	[redacted]	[redacted]	[redacted]	[redacted]	[redacted]	[redacted]
[redacted]	[redacted]	[redacted]	[redacted]	[redacted]	[redacted]	[redacted]	[redacted]

Table 6 Comparison of the Measured and Predicted Temperatures for 32 kW Heat Load with Finned Side Heat Shields

[redacted]

	[redacted]			[redacted]			[redacted]
[redacted]	[redacted]		[redacted]		[redacted]		[redacted]
[redacted]	[redacted]		[redacted]		[redacted]		[redacted]
[redacted]	[redacted]		[redacted]		[redacted]		[redacted]
[redacted]	[redacted]		[redacted]		[redacted]		[redacted]
[redacted]	[redacted]		[redacted]		[redacted]		[redacted]

	[redacted]			[redacted]			[redacted]
[redacted]	[redacted]		[redacted]		[redacted]		[redacted]
[redacted]	[redacted]		[redacted]		[redacted]		[redacted]
[redacted]	[redacted]		[redacted]		[redacted]		[redacted]
[redacted]	[redacted]		[redacted]		[redacted]		[redacted]
[redacted]	[redacted]		[redacted]		[redacted]		[redacted]

	[redacted]			[redacted]			[redacted]
[redacted]	[redacted]		[redacted]		[redacted]		[redacted]
[redacted]	[redacted]		[redacted]		[redacted]		[redacted]
[redacted]	[redacted]		[redacted]		[redacted]		[redacted]
[redacted]	[redacted]		[redacted]		[redacted]		[redacted]
[redacted]	[redacted]		[redacted]		[redacted]		[redacted]

	[redacted]		[redacted]		[redacted]
[redacted]	[redacted]		[redacted]		[redacted]
	[redacted]		[redacted]		[redacted]
	[redacted]		[redacted]		[redacted]
	[redacted]		[redacted]		[redacted]
[redacted]	[redacted]		[redacted]		[redacted]

	[redacted]		[redacted]	
[redacted]	[redacted]		[redacted]	
	[redacted]		[redacted]	
	[redacted]		[redacted]	
[redacted]	[redacted]		[redacted]	

	[redacted]		[redacted]		[redacted]
[redacted]	[redacted]		[redacted]		[redacted]
	[redacted]		[redacted]		[redacted]
	[redacted]		[redacted]		[redacted]
	[redacted]		[redacted]		[redacted]
[redacted]	[redacted]		[redacted]		[redacted]

	[redacted]		[redacted]	
[redacted]	[redacted]		[redacted]	
	[redacted]		[redacted]	
	[redacted]		[redacted]	
[redacted]	[redacted]		[redacted]	

	[redacted]		[redacted]		[redacted]
[redacted]	[redacted]		[redacted]		[redacted]
	[redacted]		[redacted]		[redacted]
	[redacted]		[redacted]		[redacted]
	[redacted]		[redacted]		[redacted]
[redacted]	[redacted]		[redacted]		[redacted]

	[redacted]		[redacted]	
[redacted]	[redacted]		[redacted]	
	[redacted]		[redacted]	
	[redacted]		[redacted]	
[redacted]	[redacted]		[redacted]	

Table 6 Comparison of the Measured and Predicted Temperatures for 32 kW Heat Load with Finned Side Heat Shields (Concluded)

[redacted]

	[redacted]	[redacted]	[redacted]
[redacted]	[redacted]	[redacted]	[redacted]
[redacted]	[redacted]	[redacted]	[redacted]

[redacted]

	[redacted]	[redacted]	[redacted]
[redacted]	[redacted]	[redacted]	[redacted]
[redacted]	[redacted]	[redacted]	[redacted]

[redacted]

	[redacted]	[redacted]	[redacted]
[redacted]	[redacted]	[redacted]	[redacted]
[redacted]	[redacted]	[redacted]	[redacted]

[redacted]

[redacted]	[redacted]	[redacted]
[redacted]	[redacted]	[redacted]

[redacted]

[redacted]	[redacted]	[redacted]
[redacted]	[redacted]	[redacted]

[redacted]

[redacted]	[redacted]	[redacted]
[redacted]	[redacted]	[redacted]

[redacted]

	[redacted]	[redacted]	[redacted]
[redacted]	[redacted]	[redacted]	[redacted]
[redacted]	[redacted]	[redacted]	[redacted]

[redacted]

	[redacted]	[redacted]	[redacted]
[redacted]	[redacted]	[redacted]	[redacted]
[redacted]	[redacted]	[redacted]	[redacted]

[redacted]

	[redacted]	[redacted]	[redacted]
[redacted]	[redacted]	[redacted]	[redacted]
[redacted]	[redacted]	[redacted]	[redacted]

[redacted]

[redacted]	[redacted]	[redacted]
[redacted]	[redacted]	[redacted]

[redacted]

[redacted]	[redacted]	[redacted]
[redacted]	[redacted]	[redacted]

[redacted]

[redacted]	[redacted]	[redacted]
[redacted]	[redacted]	[redacted]

[redacted]

[redacted]

Table 7 Comparison of the Measured and Predicted Temperatures for 36 kW Heat Load with Finned Side Heat Shields

[redacted]

Table 7 Comparison of the Measured and Predicted Temperatures for 36 kW Heat Load with Finned Side Heat Shields (Concluded)

[redacted]

[redacted]

[redacted]

[redacted]

[redacted]

[redacted]

[redacted]

[redacted]

[redacted]

[redacted]

[redacted]

[redacted]

[redacted]

[redacted]

Table 8 Comparison of the Measured and Predicted Temperatures for 40 kW Heat Load with Finned Side Heat Shields

[redacted]

Table 8 Comparison of the Measured and Predicted Temperatures for 40 kW Heat Load with Finned Side Heat Shields (Concluded)

[redacted]

	[redacted]	[redacted]	[redacted]
[redacted]	[redacted]	[redacted]	[redacted]
[redacted]	[redacted]	[redacted]	[redacted]

[redacted]

	[redacted]	[redacted]	[redacted]
[redacted]	[redacted]	[redacted]	[redacted]
[redacted]	[redacted]	[redacted]	[redacted]

[redacted]

	[redacted]	[redacted]	[redacted]
[redacted]	[redacted]	[redacted]	[redacted]
[redacted]	[redacted]	[redacted]	[redacted]

[redacted]

[redacted]	[redacted]	[redacted]
[redacted]	[redacted]	[redacted]

[redacted]

[redacted]	[redacted]	[redacted]
[redacted]	[redacted]	[redacted]

[redacted]

[redacted]	[redacted]	[redacted]
[redacted]	[redacted]	[redacted]

[redacted]

	[redacted]	[redacted]	[redacted]
[redacted]	[redacted]	[redacted]	[redacted]
[redacted]	[redacted]	[redacted]	[redacted]

[redacted]

	[redacted]	[redacted]	[redacted]
[redacted]	[redacted]	[redacted]	[redacted]
[redacted]	[redacted]	[redacted]	[redacted]

[redacted]

	[redacted]	[redacted]	[redacted]
[redacted]	[redacted]	[redacted]	[redacted]
[redacted]	[redacted]	[redacted]	[redacted]

[redacted]

[redacted]	[redacted]	[redacted]
[redacted]	[redacted]	[redacted]

[redacted]

[redacted]	[redacted]	[redacted]
[redacted]	[redacted]	[redacted]

[redacted]

[redacted]	[redacted]	[redacted]
[redacted]	[redacted]	[redacted]

[redacted]

[redacted]

Table 9 Comparison of the Measured and Predicted Temperatures for 44 kW Heat Load with Finned Side Heat Shields

[redacted]

Table 9 Comparison of the Measured and Predicted Temperatures for 44 kW Heat Load with Finned Side Heat Shields (Concluded)

[redacted]

[redacted]	[redacted]	[redacted]	[redacted]
[redacted]	[redacted]	[redacted]	[redacted]

[redacted]

[redacted]	[redacted]	[redacted]
[redacted]	[redacted]	[redacted]

[redacted]

	[redacted]	[redacted]	[redacted]
[redacted]	[redacted]	[redacted]	[redacted]
[redacted]	[redacted]	[redacted]	[redacted]

[redacted]

[redacted]	[redacted]	[redacted]
[redacted]	[redacted]	[redacted]

[redacted]

	[redacted]	[redacted]	[redacted]
[redacted]	[redacted]	[redacted]	[redacted]
[redacted]	[redacted]	[redacted]	[redacted]

[redacted]

[redacted]	[redacted]	[redacted]
[redacted]	[redacted]	[redacted]

[redacted]

	[redacted]	[redacted]	[redacted]
[redacted]	[redacted]	[redacted]	[redacted]
[redacted]	[redacted]	[redacted]	[redacted]

[redacted]

[redacted]	[redacted]	[redacted]
[redacted]	[redacted]	[redacted]

[redacted]

	[redacted]	[redacted]	[redacted]
[redacted]	[redacted]	[redacted]	[redacted]
[redacted]	[redacted]	[redacted]	[redacted]

[redacted]

[redacted]	[redacted]	[redacted]
[redacted]	[redacted]	[redacted]

[redacted]

	[redacted]	[redacted]	[redacted]
[redacted]	[redacted]	[redacted]	[redacted]
[redacted]	[redacted]	[redacted]	[redacted]

+ [redacted]

[redacted]

Table 10 Comparison of the Measured and Predicted Temperatures for 32 kW Heat Load with Un-finned Side and Louvered Top Heat Shields

[redacted]

Table 10 Comparison of the Measured and Predicted Temperatures for 32 kW Heat Load with Un-finned Side and Louvered Top Heat Shields (Concluded)

[redacted]

	[redacted]	[redacted]	[redacted]
[redacted]	[redacted]	[redacted]	[redacted]
[redacted]	[redacted]	[redacted]	[redacted]

[redacted]

	[redacted]	[redacted]	[redacted]
[redacted]	[redacted]	[redacted]	[redacted]
[redacted]	[redacted]	[redacted]	[redacted]

[redacted]

	[redacted]	[redacted]	[redacted]
[redacted]	[redacted]	[redacted]	[redacted]
[redacted]	[redacted]	[redacted]	[redacted]

[redacted]

[redacted]	[redacted]	[redacted]
[redacted]	[redacted]	[redacted]

[redacted]

[redacted]	[redacted]	[redacted]
[redacted]	[redacted]	[redacted]

[redacted]

[redacted]	[redacted]	[redacted]
[redacted]	[redacted]	[redacted]

[redacted]

	[redacted]	[redacted]	[redacted]
[redacted]	[redacted]	[redacted]	[redacted]
[redacted]	[redacted]	[redacted]	[redacted]

[redacted]

	[redacted]	[redacted]	[redacted]
[redacted]	[redacted]	[redacted]	[redacted]
[redacted]	[redacted]	[redacted]	[redacted]

[redacted]

	[redacted]	[redacted]	[redacted]
[redacted]	[redacted]	[redacted]	[redacted]
[redacted]	[redacted]	[redacted]	[redacted]

[redacted]

[redacted]	[redacted]	[redacted]
[redacted]	[redacted]	[redacted]

[redacted]

[redacted]	[redacted]	[redacted]
[redacted]	[redacted]	[redacted]

[redacted]

[redacted]	[redacted]	[redacted]
[redacted]	[redacted]	[redacted]

[redacted]

[redacted]

Table 11 Comparison of the Measured and Predicted Temperatures for 32 kW Heat Load with Un-finned Side and Louvered Top Heat Shields and Slots in the Slotted Plate Fully Plugged

[redacted]

Table 11 Comparison of the Measured and Predicted Temperatures for 32 kW Heat Load with Un-finned Side and Louvered Top Heat Shields and Slots in the Slotted Plate Fully Plugged (Concluded)

[redacted]

[redacted]

[redacted]

[redacted]

[redacted]

[redacted]

[redacted]

[redacted]

[redacted]

[redacted]

[redacted]

[redacted]

[redacted]

[redacted]

Table 12 Comparison of the Measured and Predicted Temperatures for 32 kW Heat Load with Un-finned Side Heat Shields, Flat Top Heat Shield and with Slots in Slotted Plate Fully Plugged

[redacted]

	[redacted]							
	[redacted]			[redacted]			[redacted]	
[redacted]	[redacted]		[redacted]	[redacted]	[redacted]		[redacted]	
[redacted]	[redacted]		[redacted]	[redacted]	[redacted]		[redacted]	
[redacted]	[redacted]		[redacted]	[redacted]	[redacted]		[redacted]	
[redacted]	[redacted]		[redacted]	[redacted]	[redacted]		[redacted]	
[redacted]	[redacted]		[redacted]	[redacted]	[redacted]		[redacted]	
	[redacted]							
	[redacted]			[redacted]			[redacted]	
[redacted]	[redacted]		[redacted]	[redacted]	[redacted]		[redacted]	
[redacted]	[redacted]		[redacted]	[redacted]	[redacted]		[redacted]	
[redacted]	[redacted]		[redacted]	[redacted]	[redacted]		[redacted]	
[redacted]	[redacted]		[redacted]	[redacted]	[redacted]		[redacted]	
[redacted]	[redacted]		[redacted]	[redacted]	[redacted]		[redacted]	
	[redacted]							
	[redacted]			[redacted]			[redacted]	
[redacted]	[redacted]		[redacted]	[redacted]	[redacted]		[redacted]	
[redacted]	[redacted]		[redacted]	[redacted]	[redacted]		[redacted]	
[redacted]	[redacted]		[redacted]	[redacted]	[redacted]		[redacted]	
[redacted]	[redacted]		[redacted]	[redacted]	[redacted]		[redacted]	
[redacted]	[redacted]		[redacted]	[redacted]	[redacted]		[redacted]	

	[redacted]						[redacted]			
[redacted]	[redacted]		[redacted]		[redacted]		[redacted]	[redacted]		[redacted]
	[redacted]		[redacted]		[redacted]			[redacted]		[redacted]
[redacted]	[redacted]		[redacted]		[redacted]		[redacted]	[redacted]		[redacted]
	[redacted]									
[redacted]	[redacted]		[redacted]		[redacted]		[redacted]	[redacted]		[redacted]
	[redacted]		[redacted]		[redacted]			[redacted]		[redacted]
[redacted]	[redacted]		[redacted]		[redacted]		[redacted]	[redacted]		[redacted]
	[redacted]						[redacted]			
[redacted]	[redacted]		[redacted]		[redacted]		[redacted]	[redacted]		[redacted]
	[redacted]		[redacted]		[redacted]			[redacted]		[redacted]
[redacted]	[redacted]		[redacted]		[redacted]		[redacted]	[redacted]		[redacted]

Table 12 Comparison of the Measured and Predicted Temperatures for 32 kW Heat Load with Un-finned Side Heat Shields, Flat Top Heat Shield and with Slots in Slotted Plate Fully Plugged (Concluded)

[redacted]

[redacted]

[redacted]

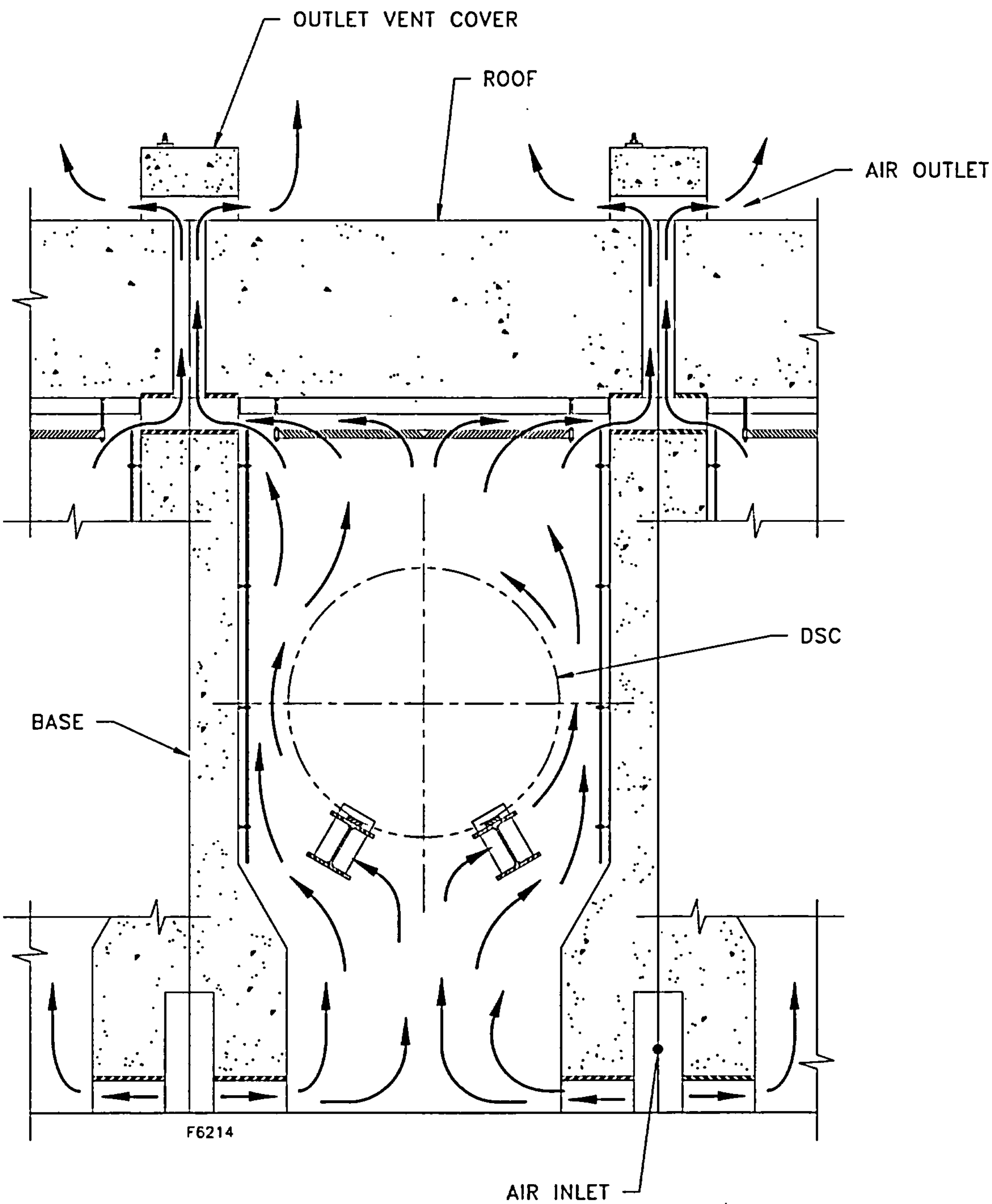

Figure 1 Air Flow in HSM-H Cavity

[redacted]

Figure 2 Dimensions of the HSM-H Mockup

[redacted]

Figure 3 Dimensions of the HSM-H Mockup, Details

[redacted]

Figure 4 Dimensions of the HSM-H Mockup, Heat Shields and Support Structure

TRANSNUCLEAR
AN AREVA COMPANY

PROJECT NO:	10494	REVISION:	0
DOCUMENT NO:	E-21625-NP	PAGE:	46 of 81

[redacted]

Figure 5 Dimensions of the DSC Mockup

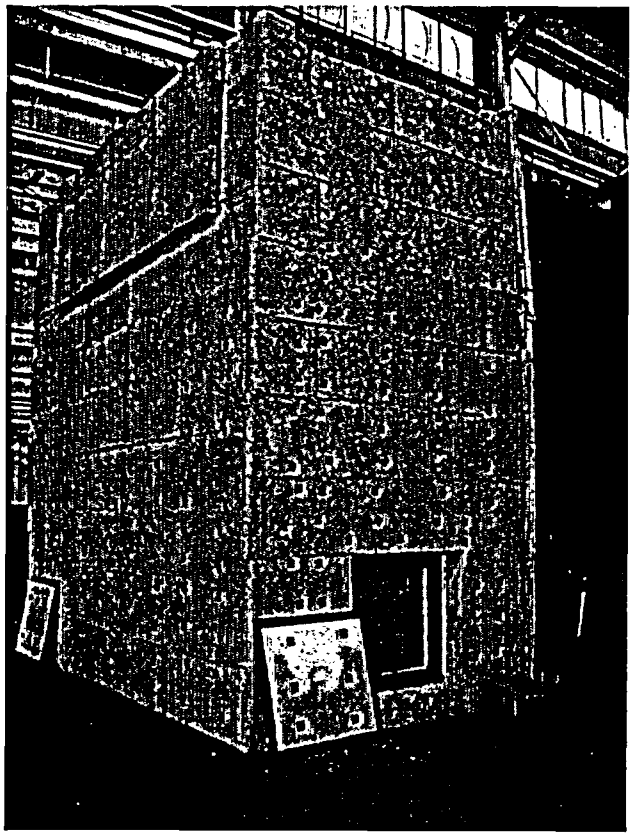

Exterior View

Interior View from Below Support Rails

Figure 6 Photos of the Constructed HSM-H Mockup

[redacted]

Figure 7 Photo of the Constructed DSC Mockup

[redacted]

Figure 8 Locations of the Thermocouples on the DSC Mockup

[redacted]

Figure 9 Locations of the Thermocouples on the HSM-H Mockup

[redacted]

Figure 10 Locations of the Thermocouples on the Heat Shields

[redacted]

Figure 11 Locations of the External Thermocouples

[redacted]

Figure 12 Schematic Setup of the Test Equipment

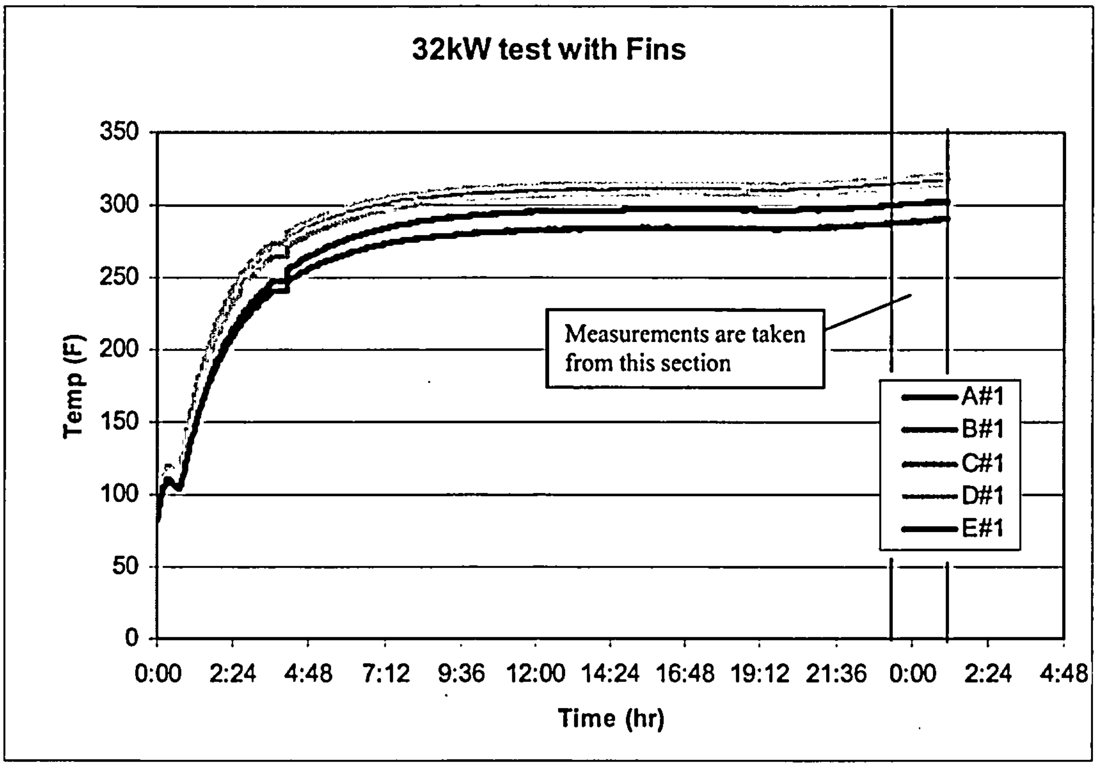

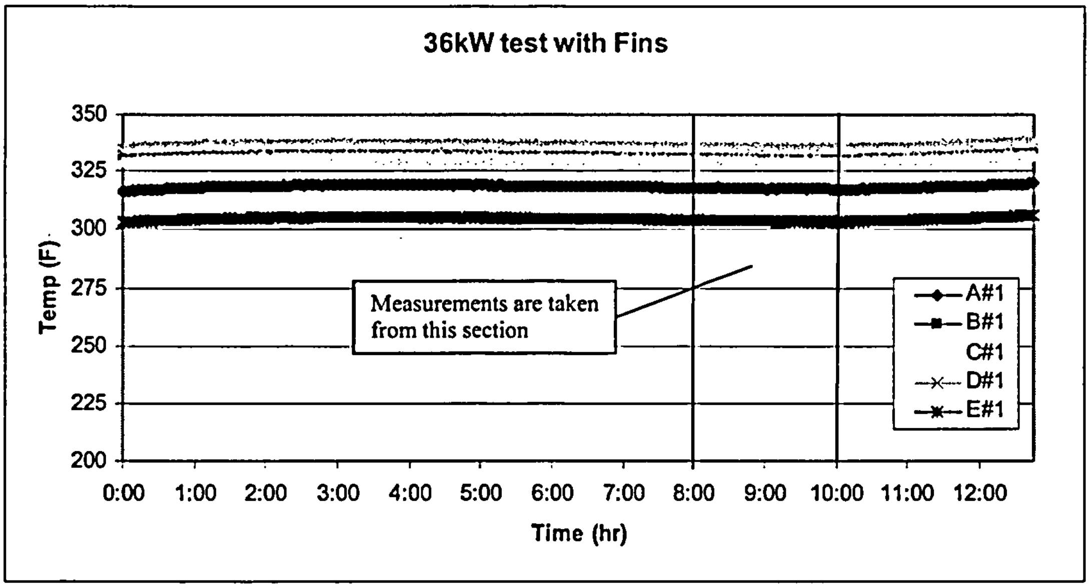

Figure 13 Typical Measured Temperature Curves for Test with Finned Heat Shields 32 kW and 36 kW Heat Loads

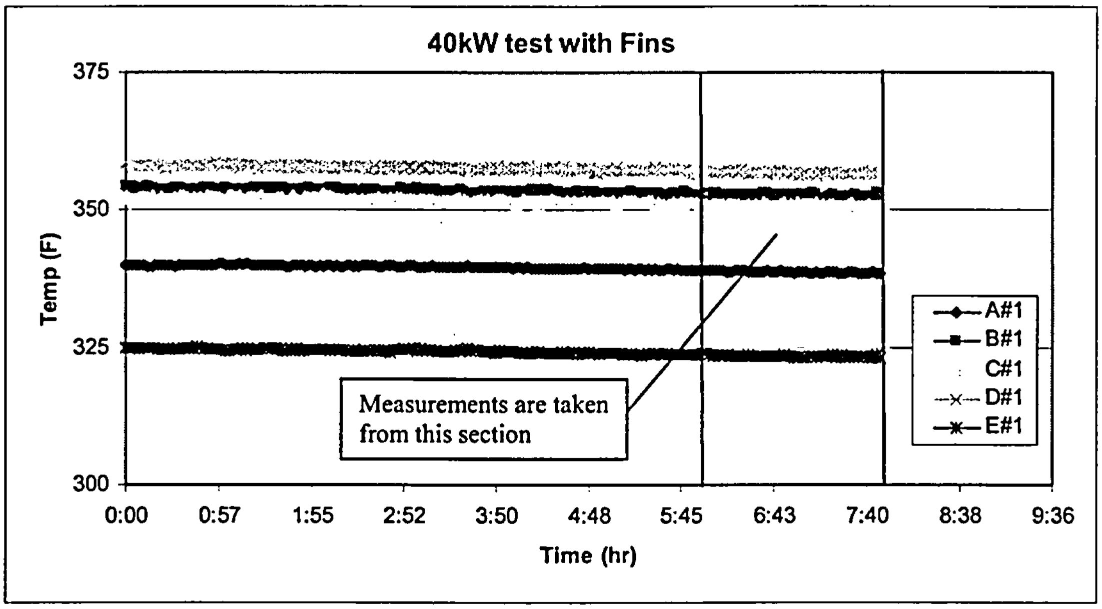

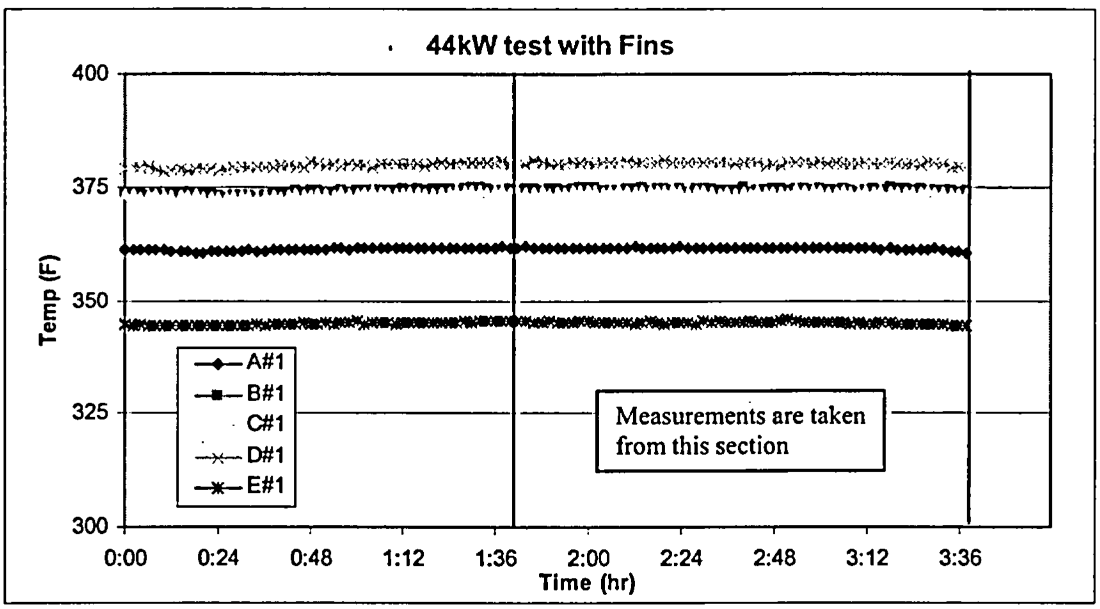

Figure 14 Typical Measured Temperature Curves for Test with Finned Heat Shields 40 kW and 44 kW Heat Loads

APPENDIX A

MEASURED DATA

Table A-1 Measured Temperatures at Steady State Condition for 32 kW Heat Load with Finned Side Heat Shield

[redacted]	[redacted]	[redacted]	[redacted]	[redacted]	[redacted]	[redacted]	[redacted]	[redacted]
[redacted]	[redacted]	[redacted]	[redacted]	[redacted]	[redacted]	[redacted]	[redacted]	[redacted]

Table A-2 Measured Temperatures at Steady State Condition for 36kW Heat Load with Finned Side Heat Shield

[redacted]	[redacted]	[redacted]	[redacted]	[redacted]	[redacted]	[redacted]	[redacted]	[redacted]
[redacted]	[redacted]	[redacted]	[redacted]	[redacted]	[redacted]	[redacted]	[redacted]	[redacted]

TRANSNUCLEAR
AN AREVA COMPANY

PROJECT NO:	10494	REVISION:	0
DOCUMENT NO:	E-21625-NP	PAGE:	59 of 81

Table A-3 Measured Temperatures at Steady State Condition for 40kW Heat Load with Finned Side Heat Shield

[redacted]

TRANSNUCLEAR
AN AREVA COMPANY

PROJECT NO:	10494	REVISION:	0
DOCUMENT NO:	E-21625-NP	PAGE:	60 of 81

Table A-4 Measured Temperatures at Steady State Condition for 44kW Heat Load with Finned Side Heat Shield

[redacted]

Table A-5 Measured Temperatures at Steady State Condition for 32 kW Heat Load with Un-finned Side Heat Shields and Louvered Top Heat Shield

[redacted]

Table A-6 Measured Temperatures at Steady State Condition for 32 kW Heat Load with Un-finned Side Heat Shields, Louvered Top Heat Shield, and Fully Plugged Slots

[redacted]

Table A-7 Measured Temperatures at Steady State Condition for 32 kW Heat Load with Un-finned Side Heat Shields, Flat Top Heat Shield, and Fully Plugged Slots

[redacted]

APPENDIX B

PREDICTED TEMPERATURES USING ANSYS MODEL AND DESIGN BASIS METHODOLOGY

Table B-1 Predicted Temperatures from ANSYS Model for 32 kW Heat Load with Finned Side Heat Shield

TC Number	Predicted Value (°F)	TC Number	Predicted Value (°F)	TC Number	Predicted Value (°F)
1	322	46	152	91	176
2	310	47	146	92	187
3	302	48	126	93	201
4	293	49	123	94	150
5	306	50	152	95	150
6	293	51	152	96	164
7	302	52	146	97	164
8	310	53	126	98	148
9	371	54	123	99	148
10	348	55	148	100	81
11	340	56	148	101	81
12	331	57	141	102	167
13	357	58	125	103	167
14	373	59	118		
15	350	60	148		
16	342	61	148		
17	333	62	141		
18	357	63	125		
19	333	64	118		
20	342	65	173		
21	350	66	156		
22	371	67	143		
23	348	68	131		
24	341	69	170		
25	331	70	153		
26	357	71	142		
27	323	72	131		
28	310	73	173		
29	302	74	117		
30	292	75	173		
31	306	76	107		
32	292	77	111		
33	302	78	107		
34	310	79	182		
35	155	80	186		
36	151	81	182		
37	148	82	117		
38	128	83	117		
39	119	84	176		
40	155	85	170		
41	151	86	175		
42	148	87	170		
43	128	88	111		
44	119	89	111		
45	152	90	111		

Table B-2 Predicted Temperatures from ANSYS Model for 36 kW Heat Load with Finned Side Heat Shield

TC Number	Predicted Value (°F)	TC Number	Predicted Value (°F)	TC Number	Predicted Value (°F)
1	339	46	153	91	179
2	326	47	147	92	191
3	318	48	125	93	207
4	308	49	122	94	152
5	323	50	153	95	152
6	308	51	153	96	167
7	318	52	147	97	167
8	326	53	125	98	149
9	392	54	122	99	149
10	366	55	149	100	76
11	358	56	149	101	76
12	348	57	141	102	168
13	376	58	124	103	168
14	393	59	116		
15	368	60	149		
16	360	61	149		
17	351	62	141		
18	377	63	124		
19	351	64	116		
20	360	65	176		
21	368	66	157		
22	391	67	143		
23	367	68	131		
24	359	69	173		
25	348	70	154		
26	377	71	141		
27	340	72	130		
28	326	73	176		
29	317	74	115		
30	306	75	176		
31	322	76	105		
32	306	77	108		
33	317	78	105		
34	326	79	187		
35	157	80	191		
36	153	81	187		
37	149	82	115		
38	127	83	115		
39	117	84	179		
40	157	85	173		
41	153	86	179		
42	149	87	173		
43	127	88	109		
44	117	89	109		
45	153	90	109		

Table B-3 Predicted Temperatures from ANSYS Model for 40 kW Heat Load with Finned Side Heat Shield

TC Number	Predicted Value (°F)	TC Number	Predicted Value (°F)	TC Number	Predicted Value (°F)
1	358	46	158	91	183
2	343	47	151	92	197
3	334	48	127	93	215
4	324	49	123	94	155
5	340	50	157	95	155
6	324	51	158	96	173
7	334	52	151	97	173
8	343	53	127	98	152
9	414	54	123	99	152
10	385	55	153	100	73
11	376	56	153	101	73
12	367	57	144	102	171
13	397	58	125	103	171
14	415	59	116		
15	387	60	153		
16	378	61	153		
17	370	62	144		
18	398	63	125		
19	370	64	116		
20	378	65	181		
21	387	66	161		
22	413	67	145		
23	385	68	132		
24	377	69	178		
25	367	70	158		
26	398	71	143		
27	358	72	132		
28	342	73	181		
29	333	74	116		
30	322	75	181		
31	340	76	104		
32	322	77	108		
33	333	78	104		
34	342	79	193		
35	160	80	198		
36	156	81	193		
37	152	82	116		
38	128	83	116		
39	118	84	185		
40	160	85	179		
41	156	86	184		
42	152	87	179		
43	128	88	109		
44	118	89	109		
45	157	90	109		

Table B-4 Predicted Temperatures from ANSYS Model for 44 kW Heat Load with Finned Side Heat Shield

TC Number	Predicted Value (°F)	TC Number	Predicted Value (°F)	TC Number	Predicted Value (°F)
1	382	46	171	91	196
2	365	47	163	92	212
3	356	48	136	93	231
4	346	49	132	94	168
5	364	50	170	95	168
6	346	51	171	96	187
7	356	52	163	97	187
8	365	53	136	98	164
9	442	54	132	99	164
10	409	55	165	100	77
11	399	56	165	101	77
12	390	57	156	102	183
13	423	58	134	103	183
14	443	59	125		
15	411	60	165		
16	402	61	165		
17	393	62	156		
18	424	63	134		
19	393	64	125		
20	402	65	195		
21	411	66	173		
22	441	67	155		
23	409	68	142		
24	400	69	192		
25	390	70	170		
26	424	71	154		
27	383	72	142		
28	365	73	196		
29	355	74	125		
30	344	75	196		
31	363	76	111		
32	344	77	116		
33	355	78	111		
34	365	79	209		
35	173	80	214		
36	169	81	209		
37	165	82	125		
38	138	83	124		
39	126	84	200		
40	173	85	193		
41	169	86	199		
42	165	87	193		
43	138	88	116		
44	126	89	116		
45	170	90	116		

Table B-5 Predicted Temperatures from ANSYS Model for 32 kW Heat Load with Un-finned Side Heat Shield and Louvered Top Heat Shield

TC Number	Predicted Value (°F)	TC Number	Predicted Value (°F)	TC Number	Predicted Value (°F)
1	312	46	142	91	156
2	313	47	137	92	170
3	311	48	112	93	191
4	285	49	108	94	145
5	291	50	140	95	145
6	285	51	142	96	164
7	311	52	137	97	164
8	313	53	112	98	141
9	365	54	108	99	141
10	363	55	135	100	62
11	365	56	136	101	62
12	334	57	129	102	144
13	343	58	110	103	144
14	368	59	102		
15	367	60	135		
16	370	61	136		
17	338	62	129		
18	344	63	110		
19	338	64	102		
20	370	65	163		
21	367	66	145		
22	365	67	127		
23	363	68	116		
24	366	69	161		
25	335	70	142		
26	343	71	127		
27	313	72	116		
28	314	73	167		
29	314	74	102		
30	285	75	167		
31	291	76	91		
32	285	77	94		
33	314	78	91		
34	314	79	184		
35	142	80	180		
36	139	81	184		
37	135	82	102		
38	113	83	102		
39	103	84	167		
40	142	85	166		
41	139	86	166		
42	135	87	166		
43	113	88	95		
44	103	89	95		
45	140	90	95		

Table B-6 Predicted Temperatures from ANSYS Model for 32 kW Heat Load with Un-finned Side Heat Shield, Louvered Top Heat Shield, and with Slots in Slotted Plate Fully Plugged

TC Number	Predicted Value (°F)	TC Number	Predicted Value (°F)	TC Number	Predicted Value (°F)
1	310	46	140	91	154
2	312	47	136	92	168
3	310	48	112	93	189
4	287	49	109	94	143
5	307	50	138	95	143
6	287	51	140	96	162
7	310	52	136	97	162
8	312	53	112	98	139
9	364	54	109	99	139
10	362	55	134	100	60
11	364	56	135	101	60
12	336	57	128	102	142
13	366	58	110	103	142
14	367	59	102		
15	366	60	134		
16	369	61	135		
17	341	62	128		
18	368	63	110		
19	341	64	102		
20	369	65	162		
21	366	66	143		
22	364	67	126		
23	362	68	117		
24	365	69	159		
25	337	70	141		
26	367	71	126		
27	311	72	117		
28	312	73	165		
29	313	74	105		
30	287	75	165		
31	307	76	92		
32	287	77	95		
33	313	78	92		
34	312	79	182		
35	140	80	178		
36	137	81	182		
37	134	82	105		
38	113	83	104		
39	103	84	165		
40	140	85	164		
41	137	86	164		
42	134	87	164		
43	113	88	97		
44	103	89	96		
45	138	90	97		

Table B-7 Predicted Temperatures from ANSYS Model for 32 kW Heat Load with Un-finned Side Heat Shield, Flat Top Heat Shield, and with Slots in Slotted Plate Fully Plugged

TC Number	Predicted Value (°F)	TC Number	Predicted Value (°F)	TC Number	Predicted Value (°F)
1	325	46	152	91	170
2	326	47	146	92	175
3	318	48	120	93	169
4	294	49	116	94	153
5	313	50	146	95	153
6	294	51	152	96	173
7	318	52	146	97	173
8	326	53	120	98	149
9	382	54	116	99	149
10	380	55	141	100	66
11	373	56	145	101	66
12	343	57	137	102	152
13	371	58	118	103	152
14	387	59	109		
15	385	60	141		
16	379	61	145		
17	348	62	137		
18	373	63	118		
19	348	64	109		
20	379	65	169		
21	385	66	154		
22	382	67	135		
23	380	68	124		
24	375	69	166		
25	344	70	152		
26	372	71	135		
27	325	72	124		
28	326	73	162		
29	322	74	112		
30	294	75	162		
31	313	76	99		
32	294	77	102		
33	322	78	99		
34	326	79	164		
35	147	80	156		
36	147	81	164		
37	143	82	112		
38	121	83	111		
39	110	84	159		
40	147	85	158		
41	147	86	155		
42	143	87	158		
43	121	88	104		
44	110	89	102		
45	146	90	104		

APPENDIX C

MEASURED INSULATION EMISSIVITY

Table C-1 Summary of the Emissivity Measurements for Insulation Materials

Emissivity Measurement for Thermafiber (Mineral Wool)

Sample A		Sample B		Sample C		Sample D	
Temp (°F)	ε	Temp (°F)	ε	Temp (°F)	ε	Temp (°F)	ε
81.8	0.866	85.7	0.886	82.2	0.864	80.8	0.870
180.97	0.86	183.4	0.872	180	0.866	174.7	0.856
253.23	0.851	248.6	0.863	249.1	0.862	251.5	0.843

Average	
Temp (°F)	ε
82	0.87
179	0.86
251	0.85

Emissivity Measurement for Spin-Glas®

Sample E		Sample F		Sample G		Sample H	
Temp (°F)	ε	Temp (°F)	ε	Temp (°F)	ε	Temp (°F)	ε
86.4	0.870	85.8	0.869	84.9	0.887	84.2	0.898
182.2	0.829	179.8	0.836	181	0.840	182.9	0.837
253	0.818	251.3	0.833	249.9	0.836	249.5	0.830

Average	
Temp (°F)	ε
85	0.89
182	0.84
251	0.83

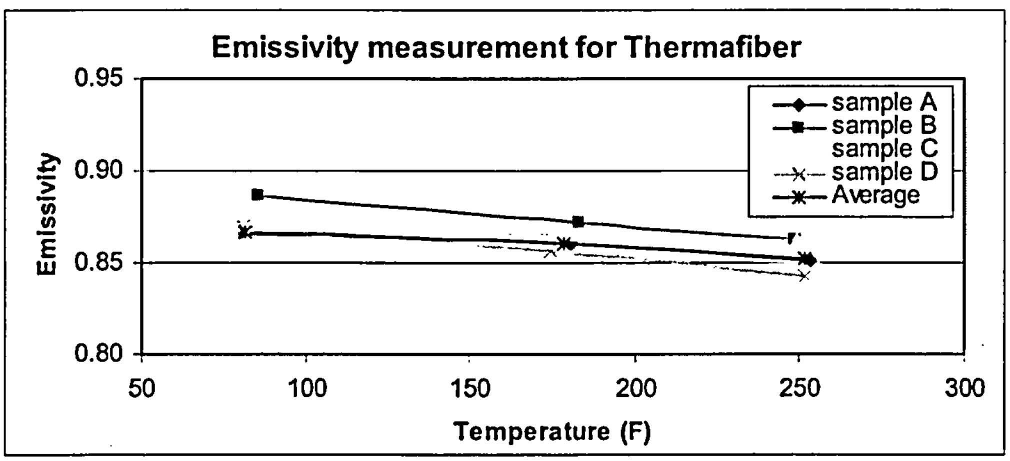

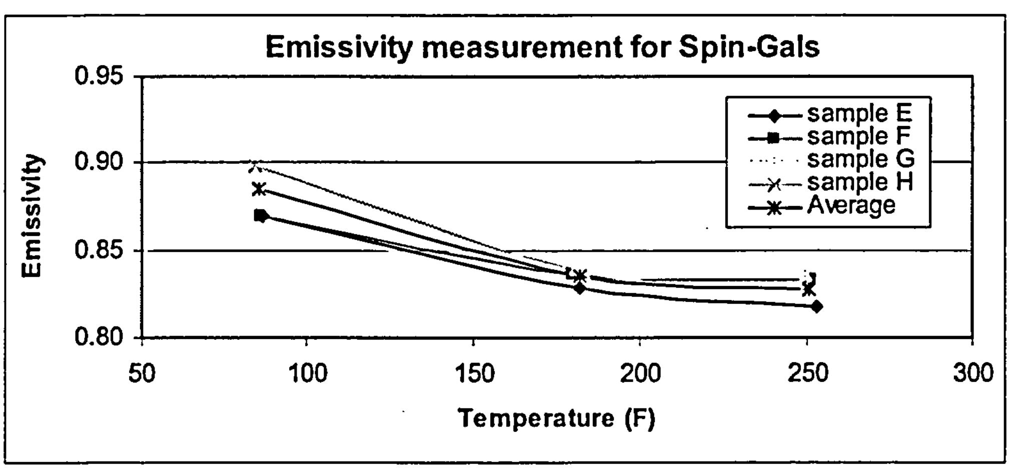

APPENDIX D

TECHNICAL DATA FOR INSULATION MATERIALS, SPIN-GLAS® AND THERMAFIBER®

JM Johns Manville

Pipe & Equipment Insulations

800 Series Spin-Glas®

Fiber Glass Duct and Equipment Insulation

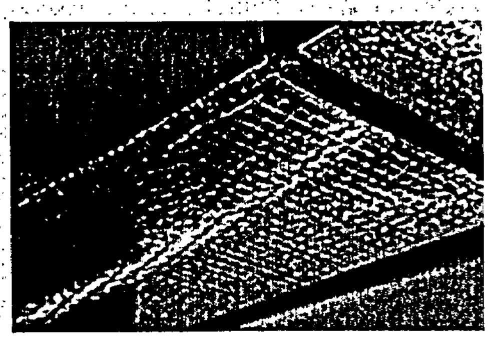

Operating Temperature Limit: Up to 450°F (232°C)

Description

800 Series Spin-Glas duct and equipment insulation is manufactured from inorganic glass fibers bonded together with thermosetting resin. 800 Series Spin-Glas is available plain or faced in a variety of densities for use on systems which operate up to 450°F (232°C). For faced products, surface temperature should not exceed 150°F (66°C). AP or FSK vapor retarder faced material meets the requirements of NFPA 90A and 90B. Types 813, 814, 815 and 817 provide neat, square corners for an excellent finished appearance on duct and equipment systems. Spin-Glas can be readily cut with an ordinary knife and secured utilizing mechanical fasteners and/or adhesives.

Uses

800 Series Spin-Glas can be used in plain or faced form to insulate heating ducts and equipment. Faced 800 Series Spin-Glas is designed for systems which operate below ambient temperatures where vapor barrier protection is required. 800 Series Spin-Glas is ideal for application on commercial and industrial heating, air conditioning, power and process equipment. These products are not designed for use inside air distribution duct work or equipment where the insulation will be directly exposed to an air stream. On systems operating below ambient temperatures, all seams should be tightly sealed with quality ASJ, Foil, or FSK tapes depending on the desired finish.

Specification Compliance

Type	812	813	814	815	817
ASTM C 612 Type IA		X	X	X	X
ASTM C 612 Type IB		X	X	X	X
ASTM C 553, Type III (Plain material only)	X				
HH-I-558C (Replaces HH-I-558B) Form B, Type I, Class 7	X	X	X	X	
ASTM E 84, UL 723, NFPA 255 CAN/ULC S102-M88 FHC 25/50, Surface Burning Characteristics (Composite)	X	X	X	X	X
NRC 1.36 MIL-I-24244C ASTM C 795 (Cleburne Material Only)	X	X	X	X	X
State of California, Title 20	X	X	X	X	X
Canada: CGSB 51-GP-10M	X	X	X	X	X
ASTM C 1136, Type I	AP Facing				
Type II	AP & FSK Facing				
(Replaces HH-B-100B Type I & II)					
NFPA 90A & 90B, FHC 25/50 & Limited Combustibility					
ISO 9000 (ANSI/ASQC 90) Certification					

Thermal Conductivity ("k")

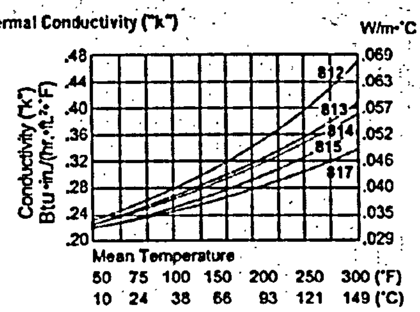

Type	812	813	814	815	817
"k" @ 75°F mean	.24	.23	.23	.22	.22
"k" @ 24°C mean	.035	.033	.033	.032	.032

Physical Properties

Temperature limit (maximum)	
Unfaced	450°F (232°C)
Faced—unfaced side	450°F (232°C)
—faced side	150°F (66°C)
Moisture sorption	Less than 5.0% by weight
Alkalinity	Less than 0.6% expressed as Na_2O
Corrosivity	Does not accelerate
Odor	None
Shrinkage	None
Resistance to fungi and bacteria	Does not breed or promote
Moisture vapor transmission—FSK & AP	0.02 perms max.

JM Johns Manville

Heat Transfer Tables
814 Series Spin-Glas® Board
Bottom of Tank or Duct

Plain or AP Facing

Ambient Temperature = 75°F   Wind = 0

Insulation Thickness (inches)	Operating Temperature (°F) 50		100		150		200		250		300		350		400		450	
	HG	ST	HL	ST	HL	ST	HL	ST	HL	ST	HL	ST	HL	ST	HL	ST	HL	ST
Bare	[illegible]	50	31	100	113	150	215	200	338	250	484	300	655	350	855	400	1087	450
½	[illegible]	68	9	82	28	96	49	110	74	124	103	140	136	156	172	174	215	192
1	[illegible]	71	5	79	16	87	28	96	42	105	88	115	76	125	98	137	120	149
1½	[illegible]	72	3	78	11	84	20	90	29	97	40	104	53	112	67	120	83	129
2	[illegible]	73	3	77	9	82	15	87	23	92	31	98	41	104	51	111	64	118
2½	[illegible]	73	2	77	7	81	12	85	18	89	25	94	33	99	42	105	52	111
3	[illegible]	73	2	77	6	80	10	83	15	87	21	91	28	96	33	101	44	106
3½	[illegible]	74	2	76	6	79	8	82	13	86	18	89	24	93	30	97	36	102
4	[illegible]	74	1	76	4	79	8	82	12	84	16	88	21	91	27	95	33	99
4½	[illegible]	74	1	76	4	78	7	81	10	84	14	86	19	90	24	93	30	97
5	[illegible]	74	1	76	4	78	6	80	9	83	13	85	17	88	22	91	27	95
5½	[illegible]	74	1	76	3	78	6	80	9	82	12	85	16	87	20	90	24	93
6	[illegible]	74	1	76	3	78	6	80	8	82	11	84	14	86	18	89	22	92
6½	[illegible]	74	1	76	3	77	6	79	7	81	10	83	13	85	17	88	21	91
7	[illegible]	74	1	76	3	77	5	79	7	81	9	83	12	85	16	87	19	90
7½	[illegible]	74	1	76	2	77	4	79	6	80	9	82	11	84	15	86	18	89
8	[illegible]	74	1	76	2	77	4	78	6	80	8	82	11	84	14	86	17	88
8½	[illegible]	74	1	76	2	77	4	78	6	80	6	81	10	83	13	85	16	87
9	[illegible]	74	1	76	2	77	4	78	5	80	7	81	10	83	12	85	15	87
9½	[illegible]	74	1	76	2	77	3	78	5	79	7	81	9	82	12	84	14	86
10	[illegible]	74	1	76	2	77	3	78	5	79	7	81	9	82	11	84	14	86

FSK Facing or Metal Jacket

Insulation Thickness (inches)	Operating Temperature (°F) 50		100		150		200		250		300		350		400		450	
	HG	ST	HL	ST	HL	ST	HL	ST	HL	ST	HL	ST	HL	ST	HL	ST	HL	ST
Bare	[illegible]	50	31	100	113	150	216	200	338	250	484	300	655	350	855	400	1087	450
½	[illegible]	62	6	89	18	113	36	137	54	162	76	189	100	217	127	246	158	277
1	[illegible]	66	4	85	12	101	23	118	34	135	48	154	63	173	80	194	100	216
1½	[illegible]	68	3	83	9	96	17	109	24	122	35	136	46	151	59	169	73	186
2	[illegible]	69	2	81	7	92	13	103	20	114	28	125	35	138	46	152	57	166
2½	[illegible]	70	2	80	6	90	11	99	16	108	23	118	30	129	38	141	47	153
3	[illegible]	70	2	80	5	88	9	95	14	104	19	113	26	122	32	133	40	144
3½	[illegible]	71	1	79	5	86	8	94	12	101	17	109	22	117	28	127	35	136
4	[illegible]	71	1	79	4	85	7	92	11	99	15	106	20	113	25	122	31	131
4½	[illegible]	72	1	79	4	85	7	91	10	97	13	103	18	110	23	118	28	126
5	[illegible]	72	1	78	3	84	6	89	9	95	12	101	16	107	20	114	25	122
5½	[illegible]	72	1	78	3	83	5	88	8	94	11	99	15	105	19	112	23	119
6	[illegible]	72	1	78	3	83	5	87	8	92	10	98	14	103	17	109	21	116
6½	[illegible]	72	1	78	3	82	5	87	7	91	10	96	13	102	16	107	20	114
7	[illegible]	73	1	78	2	82	4	86	7	90	9	95	12	100	15	106	18	111
7½	[illegible]	73	1	77	2	81	4	85	6	90	8	94	11	99	14	104	17	110
8	[illegible]	73	1	77	2	81	4	85	6	89	8	93	10	98	13	103	16	108
8½	[illegible]	73	1	77	2	81	4	85	5	88	7	92	10	97	12	101	15	106
9	[illegible]	73	1	77	2	81	3	84	5	88	7	92	9	96	12	100	15	105
9½	[illegible]	73	1	77	2	80	3	84	5	87	7	91	9	95	11	99	14	104
10	[illegible]	73	1	77	2	80	3	83	5	87	6	90	8	94	11	98	13	103

Heat Loss (Gain) in BTU/hr. per square foot of surface   ST: Surface Temperature, °F

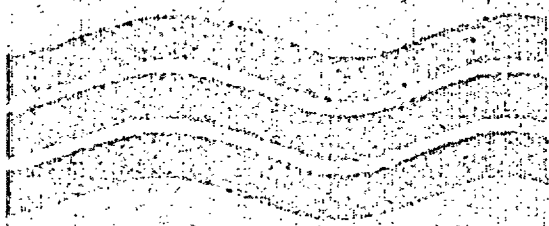

Thermafiber®

Industrial Board Insulation®

For thermal and acoustical performance in commercial and industrial applications.

Features and Benefits

- For use in continuous service up to 1200°F (649°C).
- Exceptional thermal performance and resiliency.
- Dimensionally stable at elevated temperatures with very low lineal shrinkage.
- Excellent fire performance, noncombustible.
- Will not wick moisture, promote corrosion or conduct electricity.
- Lightweight and easy to fabricate.

General Information

THERMFIBER Industrial Board Insulation is available in five nominal densities, 4 through 12 lb./cu.ft. and meet or exceed the requirements of ASTM C 612-00. Industrial Board products are available in various thicknesses from 1" to 6", in ½" increments. Standard width is 24"; standard length is 48".*

Description

THERMFIBER Industrial Board is an economical, semi-rigid, preformed mineral fiber insulation consisting of chemically inert mineral fibers bonded with a high temperature, thermosetting binder. Industrial Board is available in nominal densities from 4 to 12 lb./cu. ft. and suitable for temperatures up to 1200°F (650°C).

Applications

THERMAFIBER Industrial Board Insulation offers excellent thermal and acoustical performance in both hot and cold applications to conserve energy, maintain process temperatures, provide personnel protection, prevent condensation, and reduce noise emission and transmission.

Industrial Board Insulation may be used to insulate plant equipment such as boilers, furnaces, ovens, ducts, precipitators, tanks and other mechanical equipment operating at continuous service temperatures from sub-ambient to 1200°F.

Product Nomenclature	Nominal Density (lb)	Compliance	Max. Thickness Wabash (in.)	Max. Thickness Tacoma (in.)
Industrial Board 40	4	ASTM C 612-00, Type II	6	6
Industrial Board 60	6	ASTM C 612-00, Type III	6	4
Industrial Board 80	8	ASTM C 612-00, Type IVA	5	3
Industrial Board 100	10	ASTM C 612-00, Type IVA&B	4	2
Industrial Board 120	12	ASTM C 612-00, Type IV	4	N/A

*Non-standard sizes available

Thermal Performance

Thermal Conductivity (k)

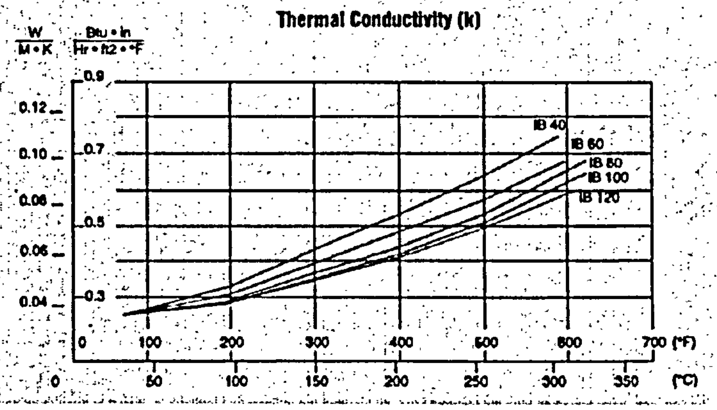

Based on measurements made in accordance with ASTM C-177 Steady State Heat Flux Measurements and Thermal Transmission Properties by Means of the Guarded Hot Plate Apparatus.

Thermafiber®

Industrial Board Insulation®

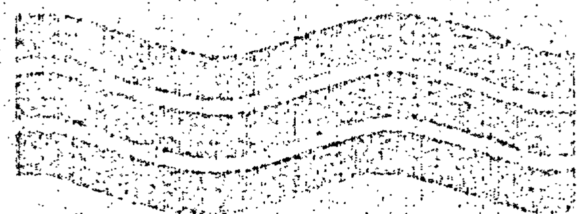

Other Information

Moisture Resistance	Adsorbs less than 1% by weight per ASTM C-553
Stress Corrosion	Complies with ASTM C-795, MIL I 24244A
Linear Shrinkage	0% at 1,050°F (551°C); <2% at 1200°F (649°C)
Melt Point	>2000° F (1093°C)
Combustibility	Rated noncombustible as defined by NFPA 220 when tested in accordance with ASTM E-136
Surface Burning Characteristics	Flame spread 15; Smoke developed 0, per ASTM E-84

Specification Compliance

THERMAFIBER Industrial Board products comply to the following standards and specifications: ASTM E-84; ASTM E-136 (rated noncombustible as defined by NFPA Standard 220 when tested according to ASTM E136); ASTM C-177; ASTM C-411; ASTM C-518; ASTM C-553 (Federal Spec. HH-I-558B); ASTM C-612; ASTM C-1338; ASTM C-165.

Start Up Procedure

On initial start-up only, heat rise should not exceed 15°F per minute to allow binder to dissipate without excessive temperature rise. Thermal conductivity is not affected. When insulation is to be used in applications exposed to high air velocities. Adequate protection must be provided to prevent erosion of insulation. Severe vibration may cause degradation of insulation under some conditions. Contact your representative for recommendations on unusual applications.

Safety First

Follow good safety and industrial hygiene practices during handling and installing of all products and systems. Take necessary precautions and wear the appropriate personal protective equipment as needed. Read material safety data sheets and related literature on products before specification and/or installation.

General

The information presented herein represents typical or average values obtained by ASTM or other standard methods. The values will vary due to normal manufacturing variations. The person using this product must determine its suitability for a particular application.

THERMAFIBER, LLC shall not be liable for incidental and consequential damages, directly or indirectly sustained, nor for any loss caused by application of these goods not in accordance with current printed instructions or for other than the intended use. Our liability is expressly limited to replacement of defective goods. Any claim shall be deemed waived unless made in writing to us within thirty (30) days from date it was or reasonably should have been discovered.

Thermafiber®
THE NAME IN MINERAL WOOL®

www.thermafiber.com

3711 West Mill Street Wabash, IN 46992
Tel: (888) 834-2371 (219) 563-2111 Fax: (800) 294-7076

2301 Taylor Way Tacoma, WA 98421-4387
Tel: (800) 426-8127 (253) 383-1537 Fax: (800) 447-0846

APPENDIX E

HEAT LOSSES THROUGH HSM-H MOCKUP OUTER SURFACES

In the HSM-H design, the heat losses through the concrete walls are minimal. To simulate similar conditions for the mockup test, the outer surfaces of the HSM-H mockup are insulated with three layers of 4" thick Thermafiber® boards. In addition, the analytical methodology described in Section 5.1 assumes no heat losses through the HSM-H walls. The heat losses through the mockup walls are calculated to demonstrate the effectiveness of the insulation.

The calculation of heat losses is based on the temperature measurements collected from thermocouples 107 through 110. Theses thermocouples are placed 4 inch deep into the insulation boards at the locations shown in Figure 11. The following equations are used to calculate the heat loss.

$$q_{loss} = \frac{(T_{insul} - T_{ambient})}{\frac{1}{h_t} + \frac{t_o}{k_{Thermafiber}}} \cdot A$$ for the walls and roof

$$q_{loss} = \frac{(T_{floor} - 70)}{\frac{t_i}{k_{Spin-Glas}} + \frac{t_{steel}}{k_{C-Steel}} + \frac{t_{conc}}{k_{concrete}} + \frac{t_{soil}}{k_{soil}}} \cdot A_{floor}$$ for the floor

T_{insul} = Temperature from Thermocouple 107 for Roor (°F)
108 for Sidewall (°F)
109 for Front Wall (°F)
110 for Back Wall (°F)
$T_{ambient}$ = Average Temperature from Thermocouples 100, 101, and 104 (°F)
A =Surface Area (in^2)
h_t = Total Heat Transfer Coefficient = $h_{rad} + h_{conv}$ Considered to be 0.01 Btu/hr-in^2-°F for this calculation
t_o = Thickness of Thermafiber® insulation board between the thermocouple and the outer surface = 4"
t_i = Thickness of Spin-Glas® insulation board between the thermocouple and the steel base plate = 1"
t_{steel} = Thickness of the steel base plate = 0.5"
t_{conc} = Thickness of the concrete below the base plate = 12"
t_{soil} = Assumed thickness of soil to temperature of 70°F= 36"
$k_{Thermafiber}$ = Conductivity of Thermafiber® board = 0.001736Btu/hr-in^2-°F [6]
$k_{Spin-Gals}$ = Conductivity of Spin-Gals® board = 0.0018 Btu/hr-in^2-°F [5]
$k_{C-Steel}$ = Conductivity of carbon steel = 35.1 Btu/hr-ft^2-°F [11]
$k_{concrete}$ = Conductivity of concrete = 0.096 Btu/hr-in^2-°F [1 and 2]
k_{soil} = Conductivity of soil = 0.0144 Btu/hr-in^2-°F [1 and 2]

The calculated heat losses are summarized in Table E. 1. As Table E. 1 shows the total heat loss through the outer surfaces of the HSM-H mockup is less than 1% of the total heat load. It concludes that the mockup simulates reasonably the HSM-H thermal function and the assumption of no heat losses in the analytical methodology is valid.

Table E. 1 – Heat Losses through HSM-H Mockup

32 kW case	$T_{ambient}$	T_{insul}	h_t	A	q_{loss}	q_{loss}
	(°F)	(°F)	(Btu/hr-in^2-°F)	(in^2)	(Btu/hr)	(kW)
Roof	82	95	0.01	28879	162.0	0.047
Sidewall	82	84	0.01	86190	88.5	0.026
Backwall	82	84	0.01	23607	25.8	0.008
Front wall	82	83	0.01	23607	11.2	0.003
Floor	70	91	---	28879	163.8	0.048
Total					287.5	0.1

Total heat loss = 0.3%

36 kW case	$T_{ambient}$	T_{insul}	h_t	A	q_{loss}	q_{loss}
	(°F)	(°F)	(Btu/hr-in^2-°F)	(in^2)	(Btu/hr)	(kW)
Roof	71	79	0.01	28879	96.7	0.028
Sidewall	71	86	0.01	86190	523.3	0.153
Backwall	71	86	0.01	23607	149.2	0.044
Front wall	71	81	0.01	23607	100.0	0.029
Floor	70	89	---	28879	172.6	0.051
Total					869.2	0.3

Total heat loss = 0.7%

40 kW case	$T_{ambient}$	T_{insul}	h_t	A	q_{loss}	q_{loss}
	(°F)	(°F)	(Btu/hr-in^2-°F)	(in^2)	(Btu/hr)	(kW)
Roof	73	81	0.01	28879	103.8	0.030
Sidewall	73	88	0.01	86190	543.7	0.159
Backwall	73	89	0.01	23607	162.2	0.048
Front wall	73	83	0.01	23607	102.2	0.030
Floor	70	91	---	28879	166.1	0.049
Total					911.8	0.3

Total heat loss = 0.7%

44 kW case	$T_{ambient}$	T_{insul}	h_t	A	q_{loss}	q_{loss}
	(°F)	(°F)	(Btu/hr-in^2-°F)	(in^2)	(Btu/hr)	(kW)
Roof	77	86	0.01	28879	113.5	0.033
Sidewall	77	95	0.01	86190	673.1	0.197
Backwall	77	97	0.01	23607	201.0	0.059
Front wall	77	90	0.01	23607	131.0	0.038
Floor	70	97	---	28879	209.5	0.061
Total					1328.1	0.4

Total heat loss = 0.9%